

## A COLD MILKY WAY STELLAR STREAM IN THE DIRECTION OF TRIANGULUM

ANA BONACA<sup>1</sup>, MARLA GEHA<sup>1</sup>, NITYA KALLIVAYALIL<sup>1</sup>

*Draft version August 31, 2021*

### ABSTRACT

We present evidence for a new Milky Way stellar tidal stream in the direction of the Andromeda and Triangulum (M31 and M33) galaxies. Using a matched-filter technique, we search the Sloan Digital Sky Survey Data Release 8 by creating stellar density maps which probe the Milky Way halo at distances between 8 and 40 kpc. A visual search of these maps recovers all of the major known stellar streams, as well as a new stream in the direction of M31/M33 which we name the Triangulum stream. The stream spans  $0.2^\circ$  by  $12^\circ$  on the sky, or 75 pc by 5.5 kpc in physical units with a best fitting distance of  $26 \pm 4$  kpc. The width of the stream is consistent with being the tidal remnant of a globular cluster. A color magnitude diagram of the stream region shows an overdensity which, if identified as a main sequence turn-off, corresponds to an old ( $\sim 12$  Gyr) and metal-poor ( $[\text{Fe}/\text{H}] \sim -1.0$  dex) stellar population. Future kinematic studies of this and similar cold streams will provide tight constraints on the shape of the Galactic gravitational potential.

*Subject headings:* Galaxy: halo — Galaxy: structure

### 1. INTRODUCTION

Stellar streams are found throughout the galactic halos of the Milky Way, Andromeda (hereafter M31) and other nearby massive galaxies (e.g., Belokurov et al. 2006; Ibata et al. 2001; Martínez-Delgado et al. 2008). These streams are presumed to originate from disrupting dwarf galaxies or globular clusters, providing evidence that galaxies are formed, at least in part, hierarchically.

The recent discovery of numerous Milky Way stellar streams is due to wide-field photometric surveys such as the Sloan Digital Sky Survey (SDSS). Many of these streams are associated with known objects such as the tidal tail system of the Sagittarius dwarf spheroidal galaxy (Majewski et al. 2003, Belokurov et al. 2006) or with globular clusters (e.g., Palomar 5; Odenkirchen et al. 2003, Palomar 14; Sollima et al. 2011). Some streams, however, are identified as isolated features in which the progenitor object is not yet identified or has been tidally disrupted beyond recognition (e.g., Monoceros Stream, Newberg et al. 2002; Orphan Stream, Belokurov et al. 2007).

Stellar streams can extend over large physical distances and are sensitive to the strength and shape of the Galactic gravitational potential (e.g., Helmi 2004; Johnston et al. 2005; Lux et al. 2012), as well as to its ‘lumpiness’ (Carlberg 2009; Yoon et al. 2011). The GD-1 tidal stream (Grillmair & Dionatos 2006) is sufficiently nearby (10 kpc) that proper motions are available for its member stars. Koposov et al. (2010) analyzed the full, six-dimensional phase space for GD-1, placing a strong constraint on the flattening of the Milky Way potential between 10-15 kpc which is dominated by the Galactic disk. An analysis of more distant streams will provide similar constraints on the Galactic halo potential. Each individual stream provides independent constraints on the Galactic potential, thus a joint analysis of many streams provides a promising method to constrain the

full Milky Way potential.

Here we present evidence for a new Milky Way stellar stream, which we name the Triangulum stream, found in projection against M31 and M33. In §2 we discuss the SDSS data analysis and matched-filter technique. In §3, we determine the stream properties, and discuss its relationship to other Galactic substructures in §3.3.

### 2. DATA ANALYSIS

We search for stellar streams in the Sloan Digital Sky Survey Data Release 8 (Aihara et al. 2011, hereafter SDSS DR8). We select stars brighter than  $r = 22$  over the  $14,555 \text{ deg}^2$  SDSS coverage, of which  $5200 \text{ deg}^2$  is newly released imaging in the Southern Galactic hemisphere. At these magnitudes, the majority of stars belong to the Milky Way disk. Stars in substructures typically belong to different stellar populations as compared to the Milky Way disk and can be distinguished by their chemical composition and age.

Rockosi et al. (2002) first introduced the matched-filter technique in the context of Milky Way substructure searches. Matched filtering works by preferentially weighting stars, in color-magnitude space, with a higher probability of being part of a stream population. Filters used in this work are based on the globular cluster M13, whose old age and low metallicity (13.5 Gyr and  $[\text{Fe}/\text{H}] = -1.6$ ; Vandenberg 2000) are similar to other known cold stellar streams. M13 is observed by SDSS, thus no filter transformations are required.

Our filter is constructed by dividing a Hess diagram of the target population (Figure 1a) by a Hess diagram of the foreground (Figure 1b). The filter target stars are selected from the DR8 photometric catalog within a radius of  $15'$  from M13's center. The foreground population is selected locally, between  $45'$  and  $75'$  from M13. The final filter is smoothed and confined to a region following the target population's isochrone within a generous tolerance (Figure 1c), which accommodates isochrones of other commonly used globular clusters (e.g., M92).

Our approach ensures that regions in the color-magnitude diagram (CMD) with high contrast between

<sup>1</sup> Department of Astronomy, Yale University, New Haven, CT 06511; ana.bonaca@yale.edu

the target and foreground population are given the most weight in filtering. The filter is most heavily weighted near the main sequence turn-off (Figure 1c), where numerous M13 stars are present, but few Galactic stars are as blue in color. The main sequence is less weighted because of the large population of Milky Way stars present redward of the turn-off. The subgiant and giant branches are weighted the least because of the small number of M13 stars which occupy those areas of the CMD.

A total of four matched filters (in  $r$  vs.  $g-r$ ,  $g$  vs.  $g-r$ ,  $g$  vs.  $g-i$  and  $g$  vs.  $g-z$ ) were applied to the whole SDSS survey area for a distance range between 8 kpc and 40 kpc. The inner distance limit was chosen to avoid the Milky Way disk, while the outer limit is the distance at which the main sequence turnoff falls below the SDSS 95% completeness limit (Jurić et al. 2008). Each filter was applied to the full SDSS photometric sample and the resulting density maps were coadded. The left column of Figure 2 shows the final density maps for the North Galactic hemisphere, while right panels show the South Galactic hemisphere<sup>2</sup>. The SDSS footprint in the North has been extensively searched for halo substructure and is known as the “field of streams” (Belokurov et al. 2006). We recover both compact and diffuse known objects in this field. Globular clusters and dwarf galaxies are visible as small, concentrated overdensities. At a distance of 8 kpc (Figure 2, top) we detect the cold GD-1 stream, as well as the much wider signatures of the Monoceros stream and leading Sagittarius tidal arm. At a distance of 26 kpc (Figure 2, bottom) we detect the tidal tails of the Palomar 5 globular cluster and the Orphan stream. A visual search of these maps does not reveal any new stellar streams beyond those which have been published. Our method recovers streams down to the limit of the faint Lethe and Styx streams (Grillmair 2009).

Stellar density maps of the South Galactic hemisphere are shown in the right column of Figure 2, at distances of 8 kpc (top) and 26 kpc (bottom). The Sagittarius trailing tidal arm is visible at both distances. At larger latitudes we also detect a fainter stream parallel to the stronger Sagittarius tail, as discussed in Koposov et al. (2012). A visual search of the Southern maps reveals a new stream in the region of M31/M33 which we describe in detail below. No other substructure features were detected.

### 3. RESULTS

We demonstrate in Figure 2 that our search method recovers all known stellar streams thus far published. In addition, we find evidence for a new narrow stream in the direction of the M31/M33 region which we name the Triangulum stream. In § 3.3, we discuss this new stream in the context of other known substructure in this region.

#### 3.1. Physical Properties of the Triangulum Stream

The Triangulum stream is long and very narrow (Figure 3a). To ensure that the feature is indeed a stellar overdensity, we show the dust extinction (Figure 3b; Schlegel et al. 1998) and number counts of blue SDSS galaxies (Figure 3c) in the stream region. Neither dust nor galaxies show an overdensity in the stream region.

<sup>2</sup> Our SDSS DR8 stellar density maps are available at <http://www.astro.yale.edu/abonaca/research/halo.html>

TABLE 1  
TRIANGULUM STREAM PROPERTIES

Property	Value
RA (deg) <sup>a</sup>	[21.346, 23.975]
Dec (deg) <sup>a</sup>	[34.977, 23.201]
$l$ (deg)	[130.756, 136.023]
$b$ (deg)	[-27.378, -38.538]
Width	0.2° (75 pc)
Length	12° (5.5 kpc)
Distance	26 ± 4 kpc
[Fe/H]	-1.0 dex
Age	12 Gyr

<sup>a</sup>Stream boundary points, see Equation 1 for a relation between RA and Dec.

The Triangulum stream is nearly linear on the sky, whose coordinates satisfy the equation:

$$\text{Dec}(\circ) = -4.4 \times \text{RA}(\circ) + 128.5 \quad (1)$$

in the range  $\text{RA} \simeq 21^\circ - 24^\circ$  (Table 1). We define a new coordinate system such that the stream runs along a  $y$ -axis. This system is an equatorial system rotated 11° counterclockwise around  $\text{RA} = 22^\circ$  and  $\text{Dec} = 32^\circ$ . A stellar density map of the stream region in this new coordinate system is shown in Figure 3d. To assess the statistical significance of this overdensity, we create a one-dimensional stellar density profile of the stream (regions  $-9^\circ < y < -6^\circ$  and  $0^\circ < y < 3^\circ$ , marked with red and blue lines on Figure 3d, respectively) extending  $|x| \leq 5^\circ$  on each side of the stream. For  $x < -1^\circ$  the stream profile is affected by the incomplete SDSS coverage. We correct for completeness by dividing the profile value with the fraction of populated pixels in each vertical bin. This procedure enables easier analysis of the stream profile, but it also introduces additional noise to the profile at  $x < -1^\circ$ . The resulting profile is shown in Figure 3e: blue and red lines are profiles of top and bottom stream regions, respectively, while the black line is their average.

The stream signal was strongest for the matched filter at 26 kpc. We show this quantitatively by fitting a Gaussian function with a constant term to the stream profile at a range of distances between 20 kpc and 30 kpc. A Levenberg–Marquardt minimization algorithm was used to solve for the mean, dispersion, and normalization of the distribution. Both the dispersion and peak of the profile are maximized at a distance of  $\sim 26$  kpc, while the mean does not depend on the distance. The height of the stream peak is  $3\sigma$  above the background noise (estimated in the region  $0.5^\circ < |x| < 5^\circ$ ) at distances 23 – 30 kpc. We adopt a distance to the stream of  $26 \pm 4$  kpc. The measured angular extent is  $\Delta x = 10'$  and  $\Delta y = 12^\circ$ , which correspond to a width of 75 pc and a length of 5.5 kpc in physical units.

We also detected a  $\sim 2\sigma$  overdensity of blue horizontal branch (BHB) stars in the lower part of the stream region ( $-9^\circ < y < -6^\circ$ ). In this box, the  $0.5^\circ$  wide strip contains on average  $7.5 \pm 0.7$  BHBs in the stream fields ( $|x| \leq 0.5^\circ$ ) and  $4.6 \pm 2.1$  BHBs in the off fields ( $0.5^\circ < |x| < 5^\circ$ ).

In general, the shape of a stellar stream traces the past orbit of its progenitor. The stream width corre-

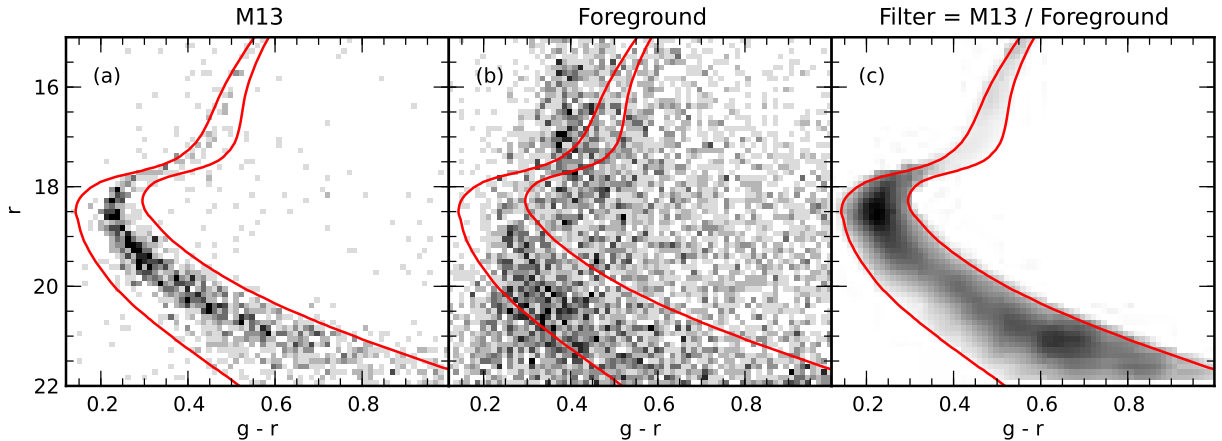


FIG. 1.— Steps in creating an M13-based filter for selection of old, metal-poor stars: the left panel shows a Hess diagram of SDSS stars detected in the inner region of globular cluster M13, while that of a surrounding area, representative of Milky Way foreground, is given in the middle panel. A ratio of the two produces the desired filter, which preferentially selects stars that are in the region of the color-magnitude diagram with the greatest contrast between M13 and Milky Way stellar populations. In order to reduce clumpiness, the filter is smoothed (right panel). The resulting filter is most heavily weighted near the main sequence turn-off. Red lines, derived from an isochrone matching the M13 population, trace the width of the filter on all three panels.

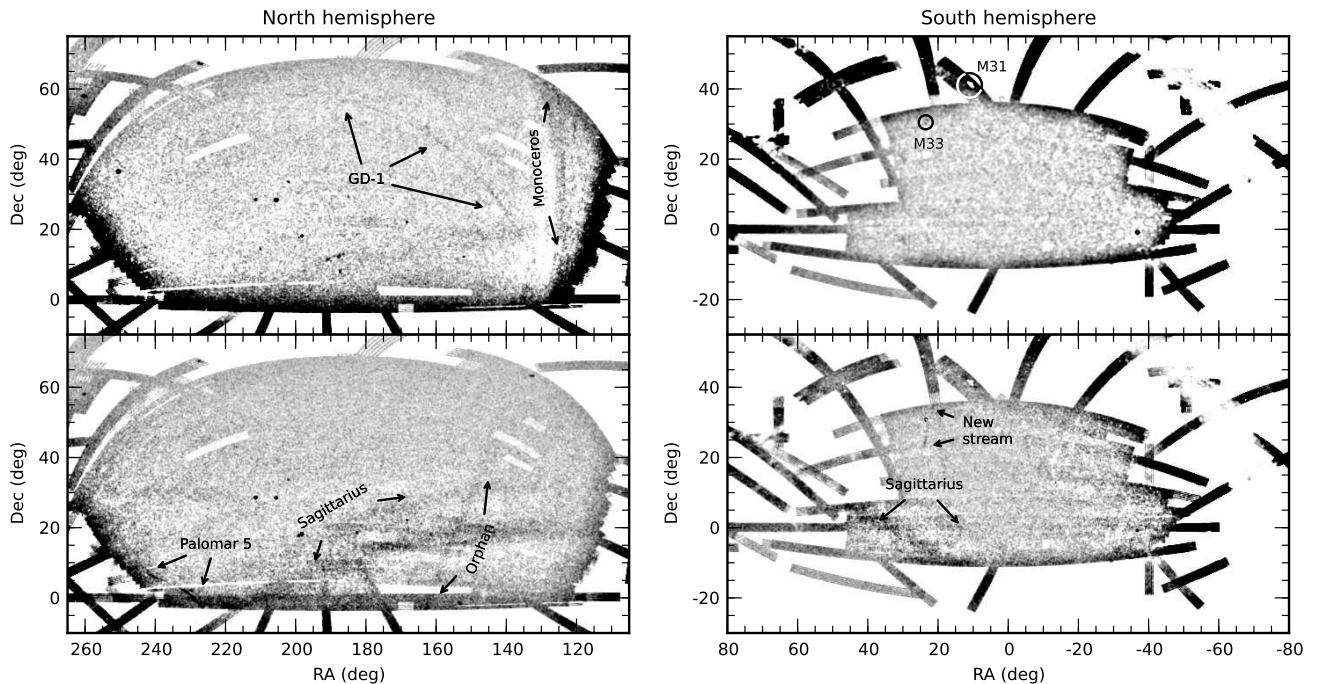


FIG. 2.— Stellar density maps obtained via matched filtering at distances of 8 kpc (top) and 26 kpc (bottom). The left columns show the SDSS footprint in the northern Galactic hemisphere, while maps on the right are in the south. The stretch is linear, with darker areas corresponding to higher stellar density regions. The most prominent features are tidal arms of the Sagittarius dwarf galaxy, bright Milky Way globular clusters, and brightest neighboring galaxies. Regions not imaged by the SDSS are shown in white. The maps are available online.

lates with progenitor mass, while the length of a stream is related to the time since the stars became unbound (Johnston & Bullock 2004). The average width of the Triangulum stream,  $\sigma = 10'$  (75 pc), is comparable to other globular cluster streams in the literature. The GD-1 stream, whose progenitor is undetected but presumed to be a globular cluster, is  $\sigma = 12'$  (35 pc; Koposov et al. 2010), while the globular cluster Pal 5 is  $\sigma = 18'$  (120 pc; Odenkirchen et al. 2003). In contrast, dwarf galaxies produce much broader streams: the Orphan stream is  $\sim 2^\circ$  wide (730 pc; Grillmair 2006; Belokurov et al. 2006), while the Sagittarius stream is  $20^\circ$  or more (7 kpc;

Belokurov et al. 2006, Majewski et al. 2003). The width of the Triangulum stream suggests that its progenitor is a globular cluster, consistent with the age and metallicity determined below.

Our estimated length for the Triangulum stream,  $12^\circ$  (5.5 kpc), is likely an underestimate given the incompleteness of the SDSS data. This is shorter, but comparable to the Palomar 5 stream ( $22^\circ$ , 9 kpc). Deeper imaging along the Triangulum stream may reveal a longer extent than detected in the SDSS data.

### 3.2. Age and Metallicity of the Triangulum Stream

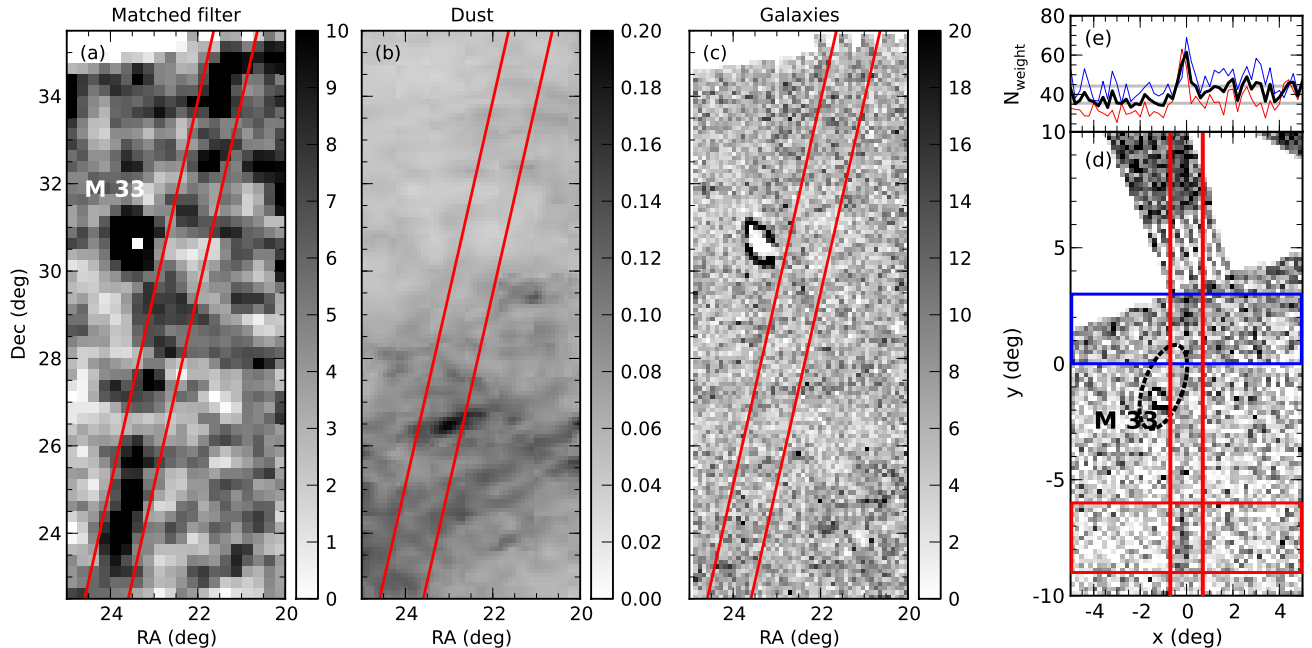


FIG. 3.— (a) Matched filter map of the Triangulum stream region in equatorial coordinates. (b) Dust map of the same region. Color scale represents reddening  $E(B - V)$ . (c) Blue galaxy number counts in the stream region. (d) Matched filter map of the wider stream region in rotated coordinates. Stream regions are boxed in blue and red, the dashed ellipse shows the extent of RGB stars around the M33 disk. Red lines on panels a-d bracket stream region. (e) 1D profiles of the stream in the top and bottom boxes from the panel (d) (blue and red, respectively) and their average (black).

We estimate the age and metallicity of the Triangulum stream using the best-fitting distance of  $26 \pm 4$  kpc. Due to the small number of stars associated with the stream, the CMD in this region is dominated by Milky Way foreground stars. We therefore follow Koposov et al. (2010) in constructing a statistically subtracted CMD. First, we create a 1D profile of all stars satisfying the color-magnitude cut  $20 < r < 22$ ,  $0.2 < g - r < 0.5$  in the stream region ( $|x| < 5^\circ$ ,  $-9^\circ < y < -6^\circ$  and  $0^\circ < z < 3^\circ$ ). This produces a well populated profile, with predominantly stream stars. Next, we fit a Gaussian to this profile to determine the central position  $x_0$  and width  $\sigma_0$ . To construct a statistically-subtracted Hess diagram, we create a 1D profile for stars in every pixel in the Hess diagram, fit the profile with a Gaussian of central position  $x_0$  and width  $\sigma_0$ , and assign each pixel the fitted Gaussian normalization. Thus, higher-value pixels correspond to regions with higher density profile in the stream region and, consequently, higher probability of being occupied by a stream rather than a foreground star.

The statistically subtracted  $r$  vs.  $g - r$  Hess diagram is noisy, but clearly shows an overdensity at  $r > 20.5$  and  $g - r < 0.5$  (Figure 4a). At a distance of 26 kpc, this overdensity corresponds to main sequence stars, and a hint of a main sequence turnoff is indeed seen. The contour of a smoothed Hess diagram is overlaid with a range of Dartmouth isochrones (Dotter et al. 2008, red isochrones on Figure 4b). The isochrones are 12 Gyr old and at a distance of 26 kpc. The left-most isochrone is the most metal-poor,  $[\text{Fe}/\text{H}] = -1.5$ , while the right-most is the most metal rich,  $[\text{Fe}/\text{H}] = -0.5$ . These values bracket the likely stream metallicity range, with the most probable value being the median  $[\text{Fe}/\text{H}] = -1.0$ . If a range of 13 Gyr isochrones is used, the inferred metallicity is lower

$[\text{Fe}/\text{H}] = -1.25$ . A range of younger and more metal rich isochrones fails to match the shape of the overdensity in the Hess diagram.

Given the proximity of the stream to the M33 galaxy, we have also overplotted a range of old and metal-poor isochrones at the distance of M33 (809 kpc; McConnachie et al. 2005) to test whether the stream could be associated with the M33 system (gray isochrones on Figure 4b). The tip of the red giant branch of that isochrone only reaches  $r = 21.5$  at  $g - r \simeq 1$ , much redder than the stream feature. We conclude that the stream is not associated with M33, but is most likely the tidal remnant of an old, metal-poor globular cluster in the Milky Way halo.

### 3.3. Relationship to Other Substructures

The Triangulum stream is in a region of sky rich with substructure. While the stream is projected against the M31/M33 system, it has no spatial overlap with any of the M31 satellites (Richardson et al. 2011) or diffuse structures discovered around M33 (marked with a dashed ellipse in Figure 3d). The M33 population is more metal-poor ( $[\text{Fe}/\text{H}] = -1.6$ ; McConnachie et al. 2010) than the Triangulum stream. Thus, we believe that Triangulum stream is a Galactic feature, unassociated with the substructure in the M31/M33 system.

The largest Milky Way feature in this region is the diffuse Triangulum-Andromeda (TriAnd) overdensity covering  $\sim 1000 \text{ deg}^2$  between  $100^\circ < l < 150^\circ$ ,  $-20^\circ > b > -40^\circ$ . It was discovered by Rocha-Pinto et al. (2004) as a smooth overdensity of M-giants in the 2MASS survey between 15 – 30 kpc. Majewski et al. (2004) refined this distance estimate using main sequence turnoff stars to 16 – 25 kpc. The mean spectroscopic metallicity of TriAnd stars is  $[\text{Fe}/\text{H}] = -0.64 \pm 0.08$ , with a CMD in-

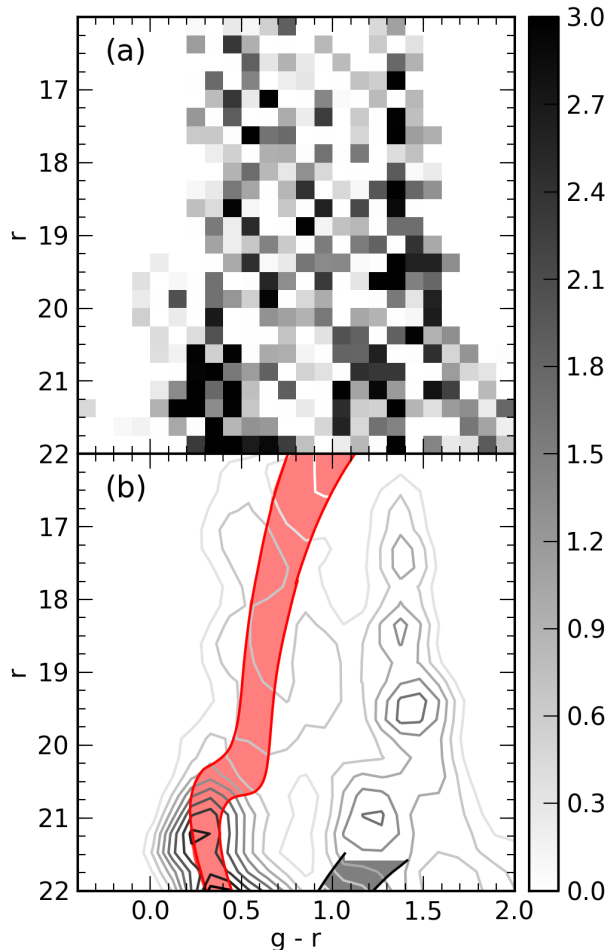


FIG. 4.— Top: Hess diagram of the stream region with statistically subtracted background. Bottom: Contours of the smoothed Hess diagram with overplotted 12 Gyr isochrones spanning a metallicity range of  $[\text{Fe}/\text{H}] = -0.5$  to  $-1.5$  at the stream distance (red) and  $[\text{Fe}/\text{H}] = -1.1$  to  $-2.1$  at the M33 distance (gray).

ferred age of 8 Gyr (Chou et al. 2011). The metallicity of TriAnd is higher than that inferred for the Triangulum stream and we estimate a population which is 4 Gyr older. Martin et al. (2007) have detected a signature of another overdensity behind the TriAnd, at heliocentric distance  $\sim 28$  kpc. Both features are far more extended than Triangulum, however, the Triangulum stream could be related to these overdensities as a localized feature at the outer edge of a much larger diffuse merger remnant. Spectroscopic and/or astrometric follow-up is required to explore this possibility.

Recently, it has been argued that the ‘bifurcation’ in the Sagittarius stream (Belokurov et al. 2006) is in fact a distinct stream with its own progenitor and kinematics (Koposov et al. 2012). The so-called Cetus stream, first discovered by Newberg et al. (2009), is fainter, thinner and more metal-poor than the Sagittarius stream. Its derived orbit is in the direction of the Triangulum stream, however, it has lower metallicity ( $[\text{Fe}/\text{H}] = -2.1$ ) and appears to be at larger heliocentric distance (34 kpc; Newberg et al. 2009). Similarly, we do not think that the Triangulum Stream is related to the Monoceros Ring/Anticenter Stellar Structure/Monoceros Stream, which is the other prominent diffuse structure in the

South. Even though the latter structure (whose origin remains controversial) has a large metallicity spread from  $[\text{Fe}/\text{H}] = -1.6$  to  $[\text{Fe}/\text{H}] = -0.4$  that could be consistent with the stream discovered here, it seems to be at much closer heliocentric distance at  $\sim 11$  kpc (Yanny et al. 2003; Crane et al. 2003; Chou et al. 2010).

#### 4. CONCLUSIONS

We have searched the SDSS DR8 photometric database for Milky Way stellar streams using a matched filtering technique. We recover all known streams in the current literature. Based on a visual search of our stellar density maps, we present evidence for a new stream discovered in the southern Galactic hemisphere in the direction of M33 which we name the Triangulum stream. We did not find any other stream-like structures in the dataset.

The Triangulum stream spans  $0.2^\circ$  by  $12^\circ$  (75 pc by 5.5 kpc) on the sky with a best fitting distance of  $26 \pm 4$  kpc. We estimate the age and metallicity of the stream via a statistically subtracted color-magnitude diagram of the region, which suggests a 12 Gyr, metal-poor ( $[\text{Fe}/\text{H}] = -1.0$ ) stellar population. The narrow width of the Triangulum stream is comparable to the GD-1 and Palomar 5 streams, from which we conclude that the Triangulum stream is also a disrupted globular cluster. While we do not observe the progenitor object, the stream extends beyond the SDSS photometric coverage. We note that the PAndAS team (McConnachie et al. 2009) has independently detected the Triangulum stream at the same sky position but at a higher significance due to deeper photometric data (M. Fardal, priv. communication).

Searches for cold stellar streams in the halo are motivated by the desire to map the Galactic gravitational potential. Further characterizing the size and shape of the Triangulum stream via deeper and more extended imaging will improve the usefulness of this stream as a Galactic halo probe. Radial velocities and proper motions of Triangulum stream stars will provide tighter constraints on the nature of its stellar populations and orbital properties, providing new constraints on the Galactic gravitational potential.

#### ACKNOWLEDGMENTS

The authors wish to thank Jeremy Bradford, Nhung Ho, Mario Jurić and Beth Willman for providing useful comments on the manuscript. We also thank Nikhil Padmanabhan for help in the early stages of this project. This work was supported by NSF grant AST-0908752 and the Alfred P. Sloan Foundation.

Funding for SDSS-III has been provided by the Alfred P. Sloan Foundation, the Participating Institutions, the National Science Foundation, and the U.S. Department of Energy Office of Science. The SDSS-III web site is <http://www.sdss3.org/>.

SDSS-III is managed by the Astrophysical Research Consortium for the Participating Institutions of the SDSS-III Collaboration including the University of Arizona, the Brazilian Participation Group, Brookhaven National Laboratory, University of Cambridge, Carnegie Mellon University, University of Florida, the French Participation Group, the German Participation Group, Harvard University, the Instituto de Astrofísica de Canarias, the Michigan State/Notre Dame/JINA Participa-

tion Group, Johns Hopkins University, Lawrence Berkeley National Laboratory, Max Planck Institute for Astrophysics, Max Planck Institute for Extraterrestrial Physics, New Mexico State University, New York Uni-

versity, Ohio State University, Pennsylvania State University, University of Portsmouth, Princeton University, the Spanish Participation Group, University of Tokyo, University of Utah, Vanderbilt University, University of Virginia, University of Washington, and Yale University.

#### REFERENCES

- Aihara, H., et al. 2011, *ApJS*, 193, 29  
Belokurov, V., et al. 2006, *ApJ*, 642, L137  
—. 2007, *ApJ*, 658, 337  
Carlberg, R. G. 2009, *ApJ*, 705, L223  
Chou, M.-Y., Majewski, S. R., Cunha, K., Smith, V. V., Patterson, R. J., & Martínez-Delgado, D. 2010, *ApJ*, 720, L5  
—. 2011, *ApJ*, 731, L30  
Crane, J. D., Majewski, S. R., Rocha-Pinto, H. J., Frinchaboy, P. M., Skrutskie, M. F., & Law, D. R. 2003, *ApJ*, 594, L119  
Dotter, A., Chaboyer, B., Jevremović, D., Kostov, V., Baron, E., & Ferguson, J. W. 2008, *ApJS*, 178, 89  
Grillmair, C. J. 2006, *ApJ*, 645, L37  
—. 2009, *ApJ*, 693, 1118  
Grillmair, C. J., & Dionatos, O. 2006, *ApJ*, 643, L17  
Helmi, A. 2004, *ApJ*, 610, L97  
Ibata, R., Irwin, M., Lewis, G., Ferguson, A. M. N., & Tanvir, N. 2001, *Nature*, 412, 49  
Johnston, K. V., & Bullock, J. S. 2004, in *Astronomical Society of the Pacific Conference Series*, Vol. 327, *Satellites and Tidal Streams*, ed. F. Prada, D. Martínez Delgado, & T. J. Mahoney, 213  
Johnston, K. V., Law, D. R., & Majewski, S. R. 2005, *ApJ*, 619, 800  
Jurić, M., et al. 2008, *ApJ*, 673, 864  
Koposov, S. E., Rix, H.-W., & Hogg, D. W. 2010, *ApJ*, 712, 260  
Koposov, S. E., et al. 2012, *ApJ*, 750, 80  
Lux, H., Read, J. I., Lake, G., & Johnston, K. V. 2012, *MNRAS*, 424, L16  
Majewski, S. R., Ostheimer, J. C., Rocha-Pinto, H. J., Patterson, R. J., Guhathakurta, P., & Reitzel, D. 2004, *ApJ*, 615, 738  
Majewski, S. R., Skrutskie, M. F., Weinberg, M. D., & Ostheimer, J. C. 2003, *ApJ*, 599, 1082  
Martin, N. F., Ibata, R. A., & Irwin, M. 2007, *ApJ*, 668, L123  
Martínez-Delgado, D., Peñarrubia, J., Gabany, R. J., Trujillo, I., Majewski, S. R., & Pohlen, M. 2008, *ApJ*, 689, 184  
McConnachie, A. W., Ferguson, A. M. N., Irwin, M. J., Dubinski, J., Widrow, L. M., Dotter, A., Ibata, R., & Lewis, G. F. 2010, *ApJ*, 723, 1038  
McConnachie, A. W., Irwin, M. J., Ferguson, A. M. N., Ibata, R. A., Lewis, G. F., & Tanvir, N. 2005, *MNRAS*, 356, 979  
McConnachie, A. W., et al. 2009, *Nature*, 461, 66  
Newberg, H. J., Yanny, B., & Willett, B. A. 2009, *ApJ*, 700, L61  
Newberg, H. J., et al. 2002, *ApJ*, 569, 245  
Odenkirchen, M., et al. 2003, *AJ*, 126, 2385  
Richardson, J. C., et al. 2011, *ApJ*, 732, 76  
Rocha-Pinto, H. J., Majewski, S. R., Skrutskie, M. F., Crane, J. D., & Patterson, R. J. 2004, *ApJ*, 615, 732  
Rockosi, C. M., et al. 2002, *AJ*, 124, 349  
Schlegel, D. J., Finkbeiner, D. P., & Davis, M. 1998, *ApJ*, 500, 525  
Sollima, A., Martínez-Delgado, D., Valls-Gabaud, D., & Peñarrubia, J. 2011, *ApJ*, 726, 47  
VandenBerg, D. A. 2000, *ApJS*, 129, 315  
Yanny, B., et al. 2003, *ApJ*, 588, 824  
Yoon, J. H., Johnston, K. V., & Hogg, D. W. 2011, *ApJ*, 731, 58